J Mol Med (2010) 88:931–939
DOI 10.1007/s00109-010-0634-1

ORIGINAL ARTICLE

The difference between rare and exceptionally rare: molecular characterization of ribose 5-phosphate isomerase deficiency

Mirjam M. C. Wamelink · Nana-Maria Grüning · Erwin E. W. Jansen · Katharina Bluemlein · Hans Lehrach · Cornelis Jakobs · Markus Ralser

Received: 24 March 2010 / Revised: 3 May 2010 / Accepted: 4 May 2010 / Published online: 25 May 2010

Abstract Ribose 5-phosphate isomerase (RPI) deficiency is an enzymopathy of the pentose phosphate pathway. It manifests with progressive leukoencephalopathy and peripheral neuropathy and belongs, with one sole diagnosed case, to the rarest human disorders. The single patient was found compound heterozygous for a RPI frameshift and a missense ($RPI^{Ala61Val}$) allele. Here, we report that two patient-derived cell lines differ in RPI enzyme activity, enzyme concentration, and mRNA expression. Furthermore, we present a transgenic yeast model, which exhibits metabolite- and enzyme-activity changes that correspond to the human syndrome and show that the decrease in RPI activity in patient cells is not fully attributable to the residue exchange. Taken together, our results demonstrate that RPI deficiency is caused by the combination of a RPI null allele with an allele that encodes for a partially active enzyme which has, in addition, cell-type-dependent expression deficits. We speculate that a low probability for comparable traits accounts for the rareness of RPI deficiency.

Keywords Ribose 5-phosphate isomerase deficiency · Rare metabolic disease · Carbohydrate metabolism · Pentose phosphate pathway

Introduction

Mutations in the mammalian genome occur non-directed. Large-scale surveys in mice reveal spontaneous mutation frequencies that vary around ~10^{-6} per locus and gamete [1]. As a consequence, every viable protein deficiency has a certain incidence. Some enzymopathies, however, are diagnosed less frequently as predicted by the natural mutation rate. This might indicate that the syndrome is not caused by homozygosis of classic null (total lack of enzyme activity) alleles. An example is triose-phosphate isomerase (TPI) deficiency. Several studies report heterozygous null-allele frequencies between 0.02 and 0.002 [2, 3]. However, since the discovery of the disorder in the 1960s, less than 100 patients have been diagnosed worldwide [2, 3]. The rare incidence of this disease is explained by homozygous lethality of TPI null alleles. The disease only manifests in individuals that are homozygous or compound heterozygous for alleles encoding enzyme specimens that are catalytically active in principal, but have defects in the formation of the enzyme's quaternary structure and stability [4, 5]. In contrast to mutations resulting in an entire loss of protein activity or presence (e.g., frameshift mutations) that can occur all along the coding sequence, such alleles are less frequent because only a few and specific residue exchanges have such effects. In TPI deficiency, with the exception of a single Hungarian family, all cases are homozygous or compound heterozygous for a missense mutation exchanging glutamic acid 105 with aspartic acid [3, 6].

Electronic supplementary material The online version of this article (doi:10.1007/s00109-010-0634-1) contains supplementary material, which is available to authorized users.

M. M. C. Wamelink · E. E. W. Jansen · C. Jakobs
Department of Clinical Chemistry,
VU University Medical Center Amsterdam,
De Boelelaan 1117,
1081 HV Amsterdam, The Netherlands

N.-M. Grüning · K. Bluemlein · H. Lehrach · M. Ralser (✉)
Max Planck Institute for Molecular Genetics,
Ihnestrasse 73,
14195 Berlin, Germany
e-mail: ralser@molgen.mpg.de

Ribose-5-phosphate isomerase deficiency is a defect of the pentose phosphate pathway (PPP) and with one single diagnosed case, the rarest possible disease. The particular patient was born in 1984 and diagnosed via magnetic resonance imaging to suffer from a progressive brain white matter disease (leukoencephalopathy) with peripheral neuropathy [7]. Systematic metabolic profiling identified elevated levels of arabitol and ribitol in affected brain regions and body fluids. In a subsequent analysis, these results lead to the discovery of a defect of the PPP enzyme ribose 5-phosphate isomerase (RPI) [7, 8]. Sequencing of the RPI-encoding cDNA identified two heterozygous mutations, one is a frameshift mutation resulting in a premature termination codon (c.540delG) inherited from the patient's mother and a missense mutation (c.182-C→T) substituting an alanine for valine at codon 61. By monitoring ribulose 5-phosphate/xylulose 5-phosphate as well as ribose 5-phosphate formation in fibroblast extracts, it was concluded that patient cells are deficient for ribose 5-phosphate isomerase activity [8]

However, since these reports published in 1999 [7] and 2004 [8], and despite the knowledge that ribitol and arabitol levels function as disease biomarkers, no further RPI patients have been identified. Because of the theoretical number of randomly occurring RPI null alleles and the strong phenotype of the patient, one would predict a higher rate of diagnoses. These observations questioned a classic enzyme loss as the genetic basis for RPI deficiency. To gain new insights into the molecular etiology of this disease, we analyzed the RPI enzyme and metabolite content as well as RPI enzyme activity in two patient-derived cell lines and a transgenic yeast model. Reduction of RPI activity in yeast caused similar changes in polyol profiles as found in the patient. However, we detected only a partial influence of the Ala61Val residue exchange on this phenotype. Instead, we find a strong and cell-type-dependent reduction of RPI mRNA expression in patient cells. These results confirm reduced overall RPI enzyme activity as the cause for the metabolic defects of RPI deficiency. However, they propose a compound-heterozygous combination of two alleles, one encoding for a null allele and the other for a partially active enzyme with cell-type-dependent expression deficits, as the molecular cause for this unique case.

Materials and methods

Plasmid generation

The generation of plasmids p416GPD-RPI (containing the human Rpi1 coding sequence under control of the *GPD1* promoter and *URA3* as marker) and p413GPD-RPI (with *HIS3* as marker) was reported previously [9]. To generating an $RPI^{Ala61Val}$ expression plasmid, the 182C→T transition was induced by generating two partial PCR products using primer pairs RPI-fwd-*Bam*HI/$RPI^{Ala61Val}$-rev and $RPI^{Ala61Val}$-fwd/RPI-rev-*Xho*I (Table 1). The two PCR products were gel-purified, combined, and used as template for a second PCR using the primer pair RPI-fwd-*Bam*HI/RPI-rev-*Xho*I. The product was digested with the restriction endonucleases *Bam*HI/*Xho*I and ligated into the equally treated expression vector p413GPD [10]. The plasmid p413CYC-RPI, designed for low-level expression of RPI, was generated by isolating the RPI-encoding *Bam*HI/*Xho*I fragment from p416GPD-RPI and ligating it into the *Bam*HI/*Sal*I sites of p413CYC. p413CYC and p413GPD differ only in the yeast promoter (*GPD1*, *CYC1*) sequence [10]. A plasmid for expression of 6xHIS tagged *Escherichia coli* transketolase (pRSET-TKL) was generated by amplifying the *E. coli* transketolase B gene from XL1blue genomic DNA using primer pairs TKL-*Bam*HI-fwd and TKL-*Xho*I-rev. The product was treated with *Bam*HI and *Xho*I and cloned into the T7 expression vector pRSET-A (Invitrogen). All generated plasmids were verified by sequencing.

Table 1 DNA primer sequences

Name	Sequence in 5′–3′ direction
RPI-fwd-*Bam*HI	GAGGATCCATGTCCAAGG CCGAGGAG
$RPI^{Ala61Val}$-rev	AGGATGAGCTGGCGGACC TGG AAGGAA
$RPI^{Ala61Val}$-fwd	TTCCTTCCAGGTCCGCCA GCTCATCCT
RPI-rev-*Xho*I	TATCTCGAGTCAACAGAA AGGCTTCTC
RPI-qPCR1-fwd	ATTGTCCATGCTGTGCAGCG
RPI-qPCR1-rev	GATCACTGAGGGTCAAGCCA
RPI-qPCR2-fwd	AGTGCTGGGAATTGGAAGTG
RPI-qPCR2-rev	CCTGGAAGGAAGTGGGAATA
RPI-qPCR3-fwd	GCCATCGATGGTGCTGATGAA
RPI-qPCR3-rev	TCCCCGAGATTCTTCGAATC
HPRT-qPCR-fwd	GGTGGAGATGATCTCTCA ACTTTAA
HPRT-qPCR-rev	AGGAAAGCAAAGTCTGCATTGTT
TKL-*Bam*HI-fwd	GAGGATCCGGTCGTGGTTCC CGAAAAGACCTTGCCAA
TKL-*Xho*I-rev	GTGAATTCTCAGGCACCT TTCACTCCCA

Underlined sequences indicate PCR-introduced restriction sites

Yeast strain generation and cultivation

Yeast was cultivated at 30°C in yeast-extract peptone dextrose (YPD) medium. *URA3* plasmids were counter-selected on synthetic complete media supplemented with 0.15% 5′ fluoroorotic acid (5′FOA, Fluorochem). The S288c (BY4741) derived Δ*rki1* yeast strain expressing human RPI from an *URA3* centromeric plasmid (*MAT*a *his3*Δ1 *leu2*Δ0 *met15*Δ0 *ura3*Δ0 *MET15*::*yor095c pcen-URA3-GPD1*$_{pr}$*-RPI*) was generated and transformed as described previously [9].

Growth curves of transgenic yeast strains were measured by diluting overnight cultures of freshly grown yeast strains in triplicates in 30 ml volume to an optical density $(OD)_{600}$ of 0.15. Cultures were shaken at 30°C, and cell density was measured hourly on an Ultrospec 2000 (Amersham Pharmacia) spectrophotometer.

Immunoblotting and antibodies

Proteins were extracted, separated on 12.5% SDS-PAGE gels, and transferred to nitrocellulose membranes by using a semidry electroblotter (PeqLAB) as described in [11]. Primary antibodies directed against human RPI (mouse polyclonal (ab67080), rabbit monoclonal (ab86123), and GAPDH rabbit polyclonal (ab36840)) were obtained from Abcam; design and generation of the α-TPI antibody (rabbit polyclonal) was reported earlier [12].

Relative quantification of RPI in cell extracts by multiple reaction monitoring (mass western)

Protein samples from control and patient lymphoblast as well as fibroblast cell lines were separated by 12.5% SDS-PAGE, and the region encompassing the mass range from 25 to 40 kDa (PageRuler prestained protein ladder (Fermentas) was used for size orientation) was excised. Proteins were extracted and digested with trypsin according to Kaiser et al. [13]. The peptide mixture was separated using a Zorbax 300SB-C18 (Agilent) column at a flow rate of 300 nl/min and analyzed on a QTRAP5500 (AB/Sciex) triple quadrupole mass spectrometer operating in multiple reaction monitoring (MRM) mode. Identity and specificity of peptides was verified by mascot (Matrix science) and blast (NCBI) database searches using MS/MS spectra obtained on the QTRAP instrument operating in (ion trap) enhanced product ion mode. Table 2 lists the MRM transitions used for protein quantification; more details about chromatographic separations and MS settings are given in Supplementary Table 2.

Cell culture

Human fibroblasts obtained from five control subjects without any known defects in metabolism and from the RPI-deficient individual were grown as monolayers in 175 cm^2 flasks (Nunc) in Ham F-10 medium. When confluent, the cells were washed twice with Hank's balanced salt solution (HBSS) and detached by adding 2 ml of trypsin. Subsequently, the cells were isolated by centrifugation for 6 min at 350×*g* and stored at −80°C until further preparation. Human lymphoblasts obtained from five control subjects without any known defects in metabolism and from the RPI-deficient individual were cultivated in RPMI 1640 medium. Cells were isolated by centrifugation of the complete cell solution for 6 min at 350×*g*, washed with HBSS, and stored at −80°C until further preparation.

cDNA synthesis and quantitative PCR

Lymphoblast and fibroblast total RNA was extracted using RNeasy extraction kit (Qiagen) and transcribed into cDNA using an 12–18 oligo dT primer and Moloney Murine Leukemia virus (M-*MuLV*) reverse transcriptase (NEB) following the manufacturer's instructions. Primer pairs for quantitative analysis of RPI mRNA were designed using Vector NTI software (Invitrogen) and are given in Table 1.

Real-time PCRs were performed in quadruplicates in 5 µl volume using a 2× SybrGreen master mix (Fermentas) and processed with the ABI Prism 7900HT sequence detection system (Applied Biosystems). The thermal cycling conditions were 50°C for 2 min, 95°C for 10 min, and 40 cycles of 95°C for 15 s/60°C for 1 min. Amplification plot and predicted threshold cycle (Ct) values were obtained with the Sequence Detection Software (SDS 2.1, Applied Biosystems). For each primer pair, the data were normalized to the endogenous reference gene (HPRT1, Table 1) in the respective cell line.

Table 2 MRM transitions

Protein	Peptide	*m/z*	Quantified fragment	Transition *m/z*
TPI	FFVGGNWK	477.75	2y6	477.75–660.35
TPI	VVLAYEPVWAIGTGK	801.95	2y9	801.95–928.53
RPI	IVAGYASR	418.73	2y6	418.73–624.31
RPI	FGGVVELR	438.75	2y7	438.75–729.43

Enzyme activity assay for ribose 5-phosphate isomerase

For the measurements of RPI activity, the different yeast cultures were grown in rich medium (YPD) overnight. Subsequently, cell cultures were diluted, and cultures of each strain were grown in parallel to mid-log phase. Cells were collected by centrifugation, washed, shock-frozen in liquid nitrogen, and lysed by glass beads in 300 µl HBSS. Human lymphoblasts and fibroblasts were collected by centrifugation, washed twice, and resuspended in 1 ml HBSS and sonicated three times for 10 s. The protein concentration in the supernatant was determined by the bicinchoninic acid protein assay kit (Sigma, procedure nr. TPRO-562). Protein extracts were stored at −80°C.

The activity of RPI was quantified spectroscopically by adapting a protocol from Novello et al. [14]. Twenty-five micrograms yeast or 75 µg human protein extract was dissolved in 2 ml 50 mM Tris buffer (pH 7.5) containing 0.1 mM NADH, 0.1 U ribose 5-phosphate epimerase, 0.1 U TKL, 33.6 U triose-phosphate isomerase, 5.7 U glyceraldehyde 3-phosphate dehydrogenase, 2 mM $MgCl_2$, and 0.1 mM thiamine pyrophosphate. After 30 min of equilibration, the reaction was started at 37°C by adding 6 µmol ribose 5-phosphate. RPI activity was quantified by the means of following the oxidation of NADH for 60 min by measuring the absorption at 340 nm. We determined a limit of detection at an activity of 0.1 µmol mg protein^{-1} min^{-1}. Enzymes except TKL were obtained from Sigma

Expression and purification of E. coli transketolase Plasmid pRSET-TKL was transformed into the *E. coli* strain BL21pLysS. Expression of the recombinant protein was induced in a culture growing exponentially at 37°C by adding 1 mM isopropyl β-D-thiogalactopyranoside. Protein extracts were generated by adding lysozyme and sonication; 6× HIS-tagged transketolase was batch-purified using Ni-NTA sepharose (Qiagen) following the manufacturer's instructions.

Quantitative metabolite measurements

For the measurements of sugar phosphates and polyols, yeast cultures were grown in rich medium (YPD) overnight. Subsequently, cell cultures were diluted, and two yeast cultures of each overnight culture were grown in parallel to mid-log phase. All steps of the lysate generation were carried out in a cold room at 4°C.

Sugar phosphates Cells were collected by centrifugation, washed, shock-frozen in liquid nitrogen, and lysed by glass beads in 400 µl cold HBSS containing 2% perchloric acid for immediate denaturation of protein after lysis. Samples were then stored at −20°C and thawed, and 50 µl internal standard (10 µM $^{13}C_6$-glucose-6P) was added to 50 µl of the lysate. Samples were then neutralized with 1 M phosphate buffer (pH 11.5) and centrifuged for 5 min at 21,000×*g* at 4°C. Supernatants were transferred to glass vials and capped. Calibrators of ribose 5-phosphate (r5p), xylulose/ribulose 5-phosphate (x5p), glucose 6-phosphate (g6p), sedoheptulose 7-phosphate (s7p), and 6-phospho gluconate (6pg) were included in each batch of samples and were processed as described above. Liquid chromatography tandem mass spectrometry (LC-MS/MS) analysis for quantification of sugar phosphates was carried out as described earlier [15, 16].

Polyols Cells were collected by centrifugation, washed, shock-frozen in liquid nitrogen, and lysed by glass beads in 400 µl cold methanol/HBSS (without phenol red) in a 2:1 ratio for immediate denaturation of protein after lysis. Samples were then stored at −20°C and thawed, and 20 µl internal standard (10 µM $^{13}C_4$-erythritol, 25 µM $^{13}C_2$-arabitol, and 60 µM $^{13}C_6$-sorbitol) was added to 80 µl of the lysate. Samples were then centrifuged for 5 min at 21,000×*g* at 4°C. Supernatants were transferred to glass vials and capped. Calibrators of arabitol, ribitol, xylitol, galactitol, and sorbitol were included in each batch of samples and were processed as described above. LC-MS/MS analysis for quantification of polyols was carried out as described earlier [17].

Results

Cell-type-dependent differences in RPI protein and mRNA expression levels as well as enzyme activity

We cultivated a patient-derived fibroblast and lymphoblast cell line to monitor the RPI- enzyme and mRNA content in comparison to respective control cell lines. As illustrated in Fig. 1a, via western blotting, we detected reduced RPI enzyme levels in both patient-derived cell lines. In addition, we noticed that lymphoblasts had a more intense RPI staining in general. Testing two different RPI antibodies (Abcam ab67080 polyclonal directed against full-length RPI and ab86123 monoclonal directed against an N-terminal peptide), we failed to detect the truncated version of RPI encoded by the frameshift allele (predicted MW 21 kDa). This indicates that the truncated RPI form is either not expressed or rapidly degraded. To obtain further and quantitative information on the RPI enzyme content, via MRM, we quantified tryptic peptides specific to RPI relative to the expression of TPI. Whole-cell protein extracts of patient and control cells were gel-separated; proteins of a mass range between 25 and 40 kDa were

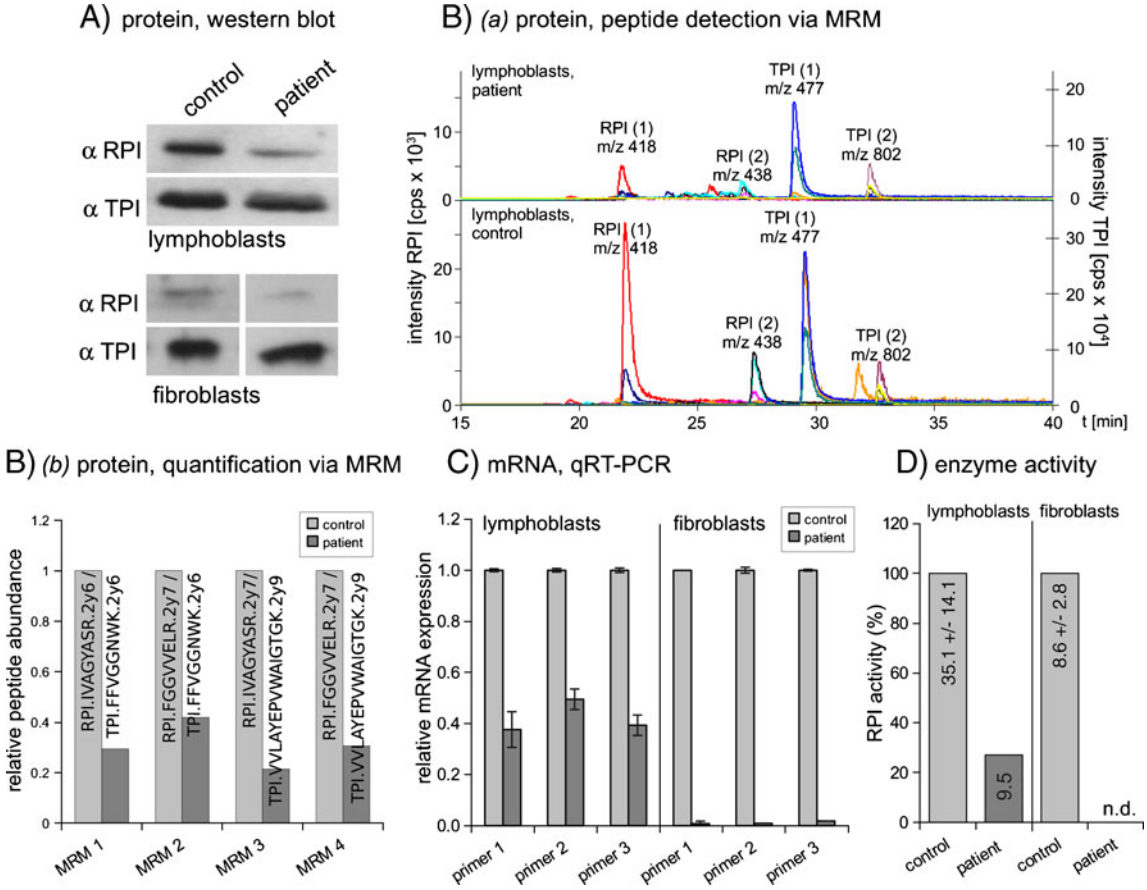

Fig. 1 RPI protein, mRNA, and activity levels are reduced, but not necessarily zero, in patient cell lines. **a** Proteins were extracted from patient and control lymphoblast as well as fibroblast cell lines and analyzed via immunoblotting. RPI protein levels were detected with an antibody directed against human RPI (ab86123); loading and quality of lysates were controlled with an antibody directed against TPI. **b** Relative quantification of RPI via multiple reaction monitoring. **b** (*a*) Chromatograms illustrate the selective detection of RPI and TPI specific peptides in tryptic digests of control and patient lymphoblasts via nano-LC-MS/MS operating in multiple reaction monitoring. *Different colors* indicate the different MRM transitions given in Suppl. Table 1. (*b*) RPI expression in control and patient lymphoblasts normalized to triose-phosphate-isomerase (*TPI*) abundance. *Bars* are labeled with the amino acid sequences/fragment ions used for quantification. **c** RPI relative mRNA concentration determined via qRT-PCR. *Bars* represent the average RPI mRNA abundance in patient cells detected with three primer pairs relative to the expression in control lymphoblasts or fibroblasts (*control*). *Error bars* indicate the standard deviation. Ct values are given in the supplementary material. **d** Overall RPI enzyme activity (substrate conversion per time) determined with a spectrophotometric enzyme-coupled RPI enzyme activity assay. Values indicate overall substrate conversion per time (μmol mg protein^{-1}min^{-1}); *bars* show normalized enzyme activity in respect to the corresponding control cell line. *n.d.* not detected (<0.1 μmol mg protein^{-1}min^{-1})

extracted and digested. As illustrated in Fig. 1b (*a*), we used two specific RPI and TPI peptides for quantification; for both, we detected multiple co-eluting transitions on the QTRAP mass spectrometer. To calculate relative alterations in RPI abundance, we normalized the peak area of the RPI-specific MRM transitions to the TPI-specific transitions. In lymphoblasts, MRM intensities of RPI-specific peptides showed in average a peak area of 30.77% when compared to control individuals (Fig. 1b (*b*)), indicating a 70% reduction of the RPI protein level. Thus, it can be concluded that the overall RPI protein levels are strongly reduced in patient cells. Furthermore, we detected strong quantitative differences in overall RPI expression between lymphoblasts and fibroblasts. In the fibroblast extracts, the RPI concentration was below the LC-MS/MS detection limit for both control and patient lines.

We continued our investigations by assaying RPI mRNA expression. We isolated total RNA from lymphoblasts and fibroblasts and transcribed poly-adenylated mRNA into cDNA. This cDNA was quality-controlled and used for a relative quantification of RPI expression via quantitative real-time PCR (qRT-PCR). We designed and tested three different qPCR primer pairs. Expression levels were normalized to human hypoxanthin phosphoribosyl transferase (HPRT) mRNA via the ΔΔCt method. All qPCR experiments demonstrated a strong decline of RPI expression in patient cells (Fig. 1c, a representative qPCR amplification plot is given in Suppl. Fig. 1). Since one of

the alleles encodes a premature stop codon [8], we had expected a decline in overall RPI mRNA due to activity of the nonsense mediated decay [18]. However, all qPCR experiments indicated a reduction of the RPI mRNA below the 50% margin. This indicates that both alleles are not expressed at wild-type levels.

Remarkably, also here, we detected strong differences between fibroblasts and lymphoblasts. In lymphoblasts, the RPI mRNA was reduced to an average of 0.42×. Although above the detection limit (Suppl. Fig. 1), RPI levels were reduced to 0.01× in patient fibroblasts. These results show that RPI mRNA expression is affected in patient cells. Furthermore, they reveal that this effect is strongly dependent on the cell type.

We continued by measuring RPI enzyme activity in both cell types quantitatively. For this, we adapted a protocol from [14], which couples ribose 5-phosphate epimerase, transketolase, triose-phosphate isomerase, and glyceraldehyde 3-phosphate dehydrogenase to determine the RPI activity via the oxidation of NADH in a classic spectrophotometer. Applying the enzyme-coupled assay, we could not detect any significant RPI activity in patient fibroblasts (Fig. 1d); however, patient lymphoblasts exhibited an activity of 28% compared to wild-type lymphoblasts. In agreement with the qPCR experiments, these results indicate that the RPI patient is not suffering from an entire loss of RPI activity. At least some cell types express the $RPI^{Ala61Val}$ enzyme and have residual activity.

Generation and validation of a yeast model for human RPI deficiency

The cell culture experiments did not allow us to distinguish if the reduction in RPI activity is primarily caused by the exchange of residue Ala61Val in the coding sequence or by the reduced expression level. Therefore, we generated a transgenic yeast model for functional analysis of RPI deficiency. As described earlier [9], we used a haploid yeast strain (BY4741) and transformed it with a plasmid encoding for human RPI under control of a strong (*GPD1*) promoter and that contained an *URA3* (counter-selectable with 5′FOA) marker. Via a single gene replacement approach, we subsequently deleted the yeast RPI orthologue *RKI1* in the human RPI expressing transformants.

To test the Δ*rki1* strain, we transformed it with a *HIS3* containing plasmid (p413GPD) and with a corresponding plasmid encoding human RPI (p413GPD-RPI). Positive transformants were spotted as 1:5 dilution series on media with and without 5' FOA. As illustrated in Fig. 2a, only yeast containing the RPI plasmid were viable on the counter-selection media. Thus, complete RPI deficiency is lethal in yeast. Furthermore, this experiment shows that human *RPI* can complement for the growth deficits caused by the lack of its yeast orthologue.

We continued our investigations by generating two new RPI expression plasmids. First, via PCR, we introduced the 182C to T transition in the single-copy centromeric vector

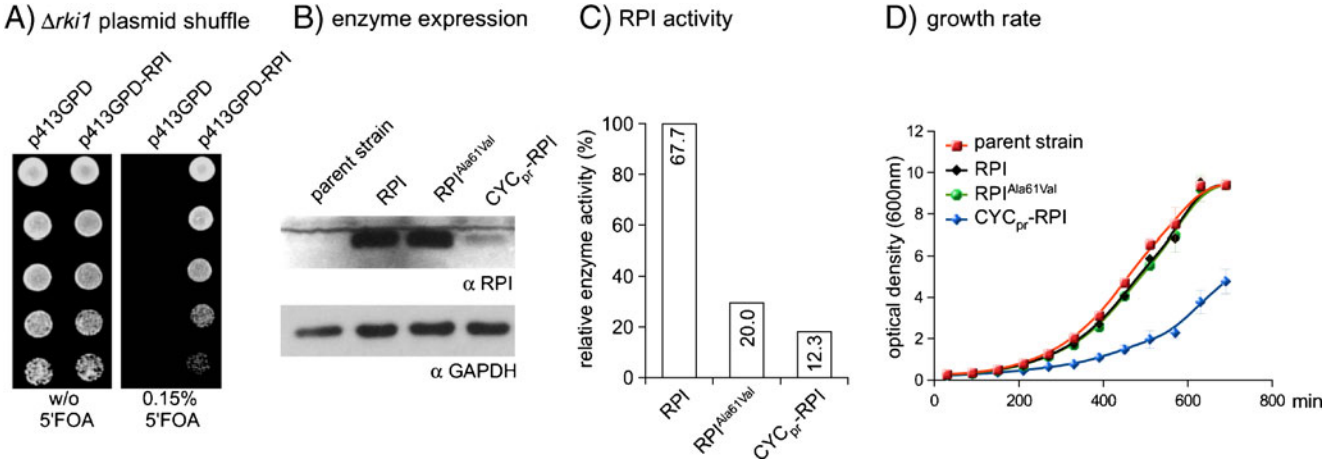

Fig. 2 A transgenic yeast model for RPI deficiency. **a** Plasmid shuffle assay: human RPI complements for its yeast orthologue Rki1p. A Δ*rki1* strain expressing human RPI from an *URA3* plasmid was transformed with either an empty or an RPI-encoding *HIS3* plasmid (p413GPD/p413GPD-RPI). Overnight cultures were spotted as 1:5 dilution series on 5′FOA media, which selects for yeast strains that have lost the *URA3* plasmid. Only transformants of the RPI-encoding vector survived. **b** Immunoblot analysis of RPI expression in transgenic yeast expressing RPI, $RPI^{Ala61Val}$ under control of the strong *GPD1* promoter, as well as RPI under control of the weak *CYC1* promoter (CYC_{pr}). Parent strain BY4741 was loaded as control; lysates were controlled with an α-GAPDH antibody. **c** Ribose 5-phosphate isomerase activity in Δ*rki1* yeast expressing RPI, $RPI^{Ala61Val}$ under control of the *GPD1* promoter, and RPI under control of the *CYC1* promoter. *Bars* illustrate normalized overall substrate conversion per time; values indicate overall substrate conversion per time (μmol mg $protein^{-1} min^{-1}$). **d** Growth of different RPI expressing yeast strains. Overnight cultures were diluted to an OD_{600} of 0.15 and grown in triplicate YPD batch cultures at 30°C. Increase in biomass was followed by measuring the OD_{600} hourly. *Error bars* indicate the standard deviation

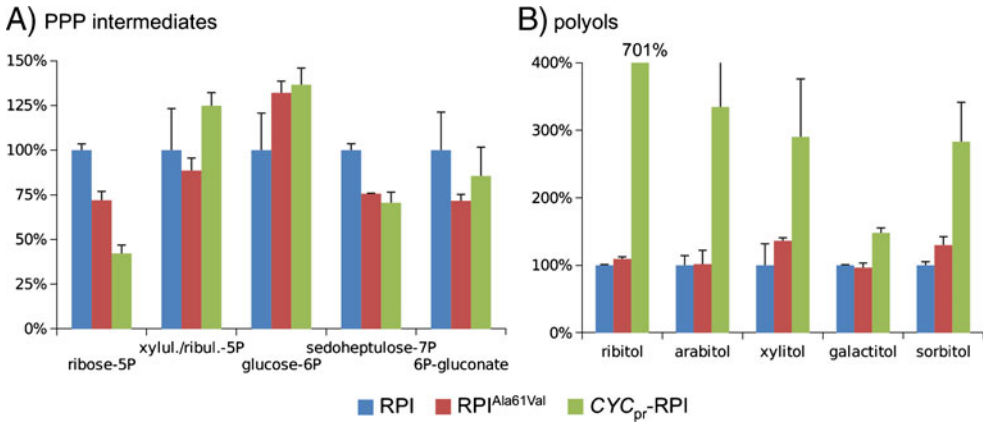

Fig. 3 Metabolic profile of transgenic RPI yeast. **a** Sugar phosphate and **b** polyole profile of wild-type (BY4741) yeast, as well as RPI expressing Δ*rki* strains determined via LC-MS/MS. Given is the concentration of the indicated metabolites normalized to the wild-type RPI expressing strain. *Error bars* indicate the standard deviation

p413GPD-RPI, resulting in an $RPI^{Ala61Val}$ expression plasmid. Second, to generate a low-level expression plasmid, we exchanged the strong *GPD1* promoter with the weak *CYC1* promoter. Along with respective controls, these plasmids were transformed into the Δ*rki1* strain and counter-selected on 5′FOA. All transformants were viable, indicating that all plasmids produced functional enzyme species.

We analyzed the RPI enzyme content in these transgenic yeast strains via immunoblotting (Fig. 2b). Yeast Rki1p expressed in the parent strain BY4741 was not detected by the antibody. Human RPI and $RPI^{Ala61Val}$ cDNA were equally expressed in yeast strains harboring the plasmids with the strong *GPD1* promoter; the CYC-promoter construct produced a significantly weaker band at the same size.

We measured enzymatic RPI activity in these strains. As shown in Fig. 2c, the $RPI^{Ala61Val}$ expressing Δ*Rki* strain exhibited 30% of the wild-type activity; the strain expressing RPI under the weak *CYC1* promoter exhibited 18% residual activity. These results show that the missense mutation leading to the exchange of alanine 61 with valine reduces the activity of RPI. However, in contrast to the previous assumption [8], the amino acid exchange per se is not sufficient to explain a RPI haploinsufficiency.

We tested the growth capacities of the different transgenic strains. They were pre-grown in YPD media and diluted to an identical biomass (measured via OD at a wavelength of 600 nm, cultures were adjusted to an OD_{600} of 0.15). Growth of triplicate batch cultures at 30°C was followed spectroscopically. As illustrated in Fig. 2d, yeast cells expressing human RPI and $RPI^{Ala61Val}$ had no obvious growth defect compared to wild-type strain. However, the strain expressing RPI under control of the weak *CYC1* promoter grew much slower. These results indicate that the $RPI^{Ala61Val}$ allele, if expressed at high levels, is sufficient to complement for the loss of yeast Rki1p and to promote cell growth at a normal rate. In contrast, low-level expression of the wild-type allele did not sufficiently compensate for the loss of this essential gene.

Transgenic RPI yeast has a metabolic profile similar to RPI deficiency

The RPI patient presented with a clear metabolic profile, which included increased ribitol and arabitol levels, as well as general differences in his polyol profile [7, 8]. These measurements led to the discovery of the genetic RPI defect [8]. However, because of the lack of comparable cases, it was not possible to exclude secondary (i.e., genetic background) effects that might have contributed or even caused this metabolic phenotype. We analyzed the polyol and sugar-phosphate pool of our transgenic yeast strains via LC-MS/MS to provide an additional and independent proof that reduced RPI activity is causal for the metabolic defects of RPI deficiency.

As illustrated in Fig. 3, yeast expressing $RPI^{Ala61Val}$ and RPI under control of the weak promoter exhibited differences in the cellular metabolite concentrations relative to yeast expressing wild-type RPI (all measured metabolite concentrations are given as Supplementary material Table 2). Analyzing sugar-phosphate intermediates of the PPP, we detected a clear decrease in ribose-5P and sedoheptulose-7P concentration (Fig. 3a). The expression of the altered RPI forms, however, had major influence on the cellular polyol pool. Polyols are sugar alcohols that can be synthesized from sugar-phosphates and were found accumulated in patient samples [8]. All addressed polyols (ribitol, arabitol, xylitol, galactitol, and sorbitol) were strongly elevated in the yeast strain expressing RPI under the weak promoter (Fig. 3b). Remarkably, the most significant metabolic changes were observed for ribitol, arabitol, and xylitol, which were increased to 300% and more. These metabolites are highly elevated in urine, plasma, and CSF of the RPI deficiency patient [8]. Therefore, these results show that the increase in polyol metabolites in the patient is indeed attributed to the reduced RPI activity. Furthermore, they indicate that the RPI expression level is very critical for the metabolic phenotype since low-level RPI expression provoked a stronger metabolic phenotype as $RPI^{Ala61Val}$ residue exchange.

Discussion

Here, we describe a detailed molecular analysis of RPI deficiency, which is to date, to our knowledge, the rarest human disease. RPI is an enzyme of the PPP and an important player of cellular carbohydrate metabolism, where it interconverts ribose-5-phosphate and ribulose-5-phosphate [14].

In humans, three enzyme defects of the PPP are associated with clinical symptoms. Glucose-6-phosphate dehydrogenase deficiency is the most common human enzyme defect and present in more than 400 million people worldwide [19]. Transaldolase deficiency, the second defect, was first described in 2001 [20] and has meanwhile been diagnosed in unrelated patients of Turkish, Arabian, Pakistani, and Polish origin [21, 22]. RPI deficiency is the third defect and appears to be very rare. At the time of the discovery of the enzyme defect [8], a loss of RPI enzyme activity was assumed to be the molecular cause of the patient's molecular and pathologic phenotype. These conclusions were supported by LC-MS/MS assays performed on patient's fibroblast extracts, which pointed to a deficiency of ribulose-5-phosphate to ribose-5 phosphate interconversion. A classic loss of enzyme activity, however, which is caused by multiple types of mutations that can occur everywhere in the RPI-encoding sequences (e.g., nucleotide insertions/deletions that result in a frame shift), would predict some occurrence of RPI cases. However, in the last 10 years, no further patients have been reported nor were there any identified in our clinical routine screening. These observations lead us to considering a more complex basis of RPI deficiency.

We analyzed two cell lines derived from the patient, lymphoblasts and fibroblasts. Semi-quantitative western blotting identified a decline in RPI concentration in both cell types, and we failed to detect the truncated form encoded by the frameshift allele. These results were confirmed by quantitative mass spectrometry, which demonstrated a decline in RPI level to around 30% of the wild-type level in lymphoblasts. Furthermore, qPCR experiments demonstrated that overall RPI mRNA expression was strongly reduced in patient cells. Surprisingly, we detected huge differences between the two studied cell lines. Whereas RPI mRNA levels were reduced to around 40% in lymphoblasts, patient fibroblasts had only about 1% of RPI mRNA compared to control fibroblasts. These results are consistent with the subsequent enzymatic assays that reported a residual RPI activity of about 30% in lymphoblasts, but an activity below the assay's detection limit in fibroblasts. Regarding these values, it remains possible that different fibroblast cell lines may vary in RPI enzyme content and activity. However, in a test experiment, four different control fibroblast lines showed RPI activities of similar range (5.8/7.3/9.1 and 12.3 nmol μg protein^{-1} min^{-1}).

Obviously, the allele encoding mutant RPI^{Ala61Val} has two defects. One causes decline in the specific enzyme activity, and the other results in a cell-type-dependent decrease in RPI mRNA expression. Future investigations are needed to clarify the mechanism underlying the mRNA expression defect. We noticed that the C→T transition is located in the first codon of exon 3. Therefore, because it is close to the splice acceptor site, this mutation could affect the maturation of RPI mRNA. Another possibility is that this mutation destroys or generates a binding site for a yet unknown regulatory molecule.

On the organismic level, cell-type dependence of the RPI defect could serve to explain a major feature of RPI deficiency. Although the PPP is ubiquitously active, the RPI patient has a neuronal phenotype. It is possible that the CNS contains more or a higher percentage of cells exhibiting the RPI expression defect. However, due to the lack of biopsy material, it was at present not possible to address this issue in experiment.

We used a yeast model to compare the effects of the amino acid exchange and reduced expression level of a wild-type allele on enzyme activity and metabolic consequences. RPI^{Ala61Val} expressing yeast had about 30% overall enzyme activity when compared to the isogenic, wild-type RPI expressing yeast strain. This residual activity was sufficient to complement for the growth defects of the Δ*Rki1* strain and comparable to the enzyme activity detected in patient's lymphoblasts. These results reveal that the extremely low RPI activity in patient's fibroblast is in large parts attributable to the low expression level of the RPI allele.

Lastly, we report the sugar-phospate and polyol profile of the RPI-deficient yeast strain. Beside concentration changes in PPP intermediate sugar phosphates, the yeast strains strongly accumulated the polyols ribitol, arabitol, and xylitol. These metabolites were strongly elevated in body fluids of the patient as well [8]. This result confirms that polyols are suitable biomarkers for RPI deficiency, a fact that might facilitate the diagnosis of further cases of RPI deficiency.

In summary, we provide evidence that defects in RPI expression are crucial for the phenotype of RPI deficiency. The expression deficit is dependent on the cell type and affects an allele which encodes for a partially active RPI enzyme. The unique patient is compound heterozygous for this allele and an RPI null allele, which encodes for a truncated RPI enzyme that was, in addition, not expressed in patient cell lines. The facts that no individual homozygous for RPI null alleles has been detected, and the *RKI1* knock-out is lethal for yeast, allows speculation that cases with a complete lack of RPI activity are not viable. Consequently, RPI deficiency is penetrating rarer as the natural occurrence of null alleles. This fact, however, does not exclude the possibility that other genetic factors, cell-

type-dependent modifiers for instance, are contributing to the rare occurrence of RPI deficiency. It is currently not certain if similar compound heterozygosities are indeed compatible with life in other genetic backgrounds.

At present, only a few genes causative for exceptionally rare genetic disorders are described. This is partly due to the fact that classic cloning and mapping techniques require multiple affected (and preferentially unrelated) individuals for identification of the disease causing gene. However, this picture may change rapidly because next-generation sequencing technologies facilitate the in-depth analyses of individual human genomes. RPI deficiency may therefore become part of a larger number of monogenic diseases that penetrate exceptionally seldom because of a complex molecular etiology.

Acknowledgments We thank our colleagues for critical reading of the manuscript, Antje Krüger, Andreas Dahl, Mirjam Blattner, and Nada Kumer for help with RNA extraction and qPCRs, Serkan Ceyhan and Yvonne Himst for help with the sugar-phosphate determination and the enzyme assays, Beata Lukaszewska-McGreal for proteomic sample preparation, and the Max Planck Institute for Molecular Genetics for funding. We declare no competing interests.

References

1. Schlager G, Dickie MM (1971) Natural mutation rates in the house mouse. Estimates for five specific loci and dominant mutations. Mutat Res 11:89–96
2. Ralser M, Nebel A, Kleindorp R, Krobitsch S, Lehrach H, Schreiber S, Reinhardt R, Timmermann B (2008) Sequencing and genotypic analysis of the triosephosphate isomerase (TPI1) locus in a large sample of long-lived Germans. BMC Genet 9:38
3. Schneider AS (2000) Triosephosphate isomerase deficiency: historical perspectives and molecular aspects. Baillières Best Pract Res Clin Haematol 13:119–140
4. Ralser M, Heeren G, Breitenbach M, Lehrach H, Krobitsch S (2006) Triose phosphate isomerase deficiency is caused by altered dimerization—not catalytic inactivity—of the mutant enzymes. PLoS ONE 1:e30
5. Orosz F, Olah J, Ovadi J (2009) Triosephosphate isomerase deficiency: new insights into an enigmatic disease. Biochim Biophys Acta 1792:1168–1174
6. Schneider A, Cohen-Solal M (1996) Hematologically important mutations: triosephosphate isomerase. Blood Cells Mol Dis 22:82–84
7. van der Knaap MS, Wevers RA, Struys EA, Verhoeven NM, Pouwels PJ, Engelke UF, Feikema W, Valk J, Jakobs C (1999) Leukoencephalopathy associated with a disturbance in the metabolism of polyols. Ann Neurol 46:925–928
8. Huck JH, Verhoeven NM, Struys EA, Salomons GS, Jakobs C, van der Knaap MS (2004) Ribose-5-phosphate isomerase deficiency: new inborn error in the pentose phosphate pathway associated with a slowly progressive leukoencephalopathy. Am J Hum Genet 74:745–751
9. Ralser M, Zeidler U, Lehrach H (2009) Interfering with glycolysis causes Sir2-dependent hyper-recombination of *Saccharomyces cerevisiae* plasmids. PLoS ONE 4:e5376
10. Mumberg D, Muller R, Funk M (1995) Yeast vectors for the controlled expression of heterologous proteins in different genetic backgrounds. Gene 156:119–122
11. Ralser M, Nonhoff U, Albrecht M, Lengauer T, Wanker EE, Lehrach H, Krobitsch S (2005) Ataxin-2 and huntingtin interact with endophilin-A complexes to function in plastin-associated pathways. Hum Mol Genet 14:2893–2909
12. Yamaji R, Fujita K, Nakanishi I, Nagao K, Naito M, Tsuruo T, Inui H, Nakano Y (2004) Hypoxic up-regulation of triosephosphate isomerase expression in mouse brain capillary endothelial cells. Arch Biochem Biophys 423:332–342
13. Kaiser P, Meierhofer D, Wang X, Huang L (2008) Tandem affinity purification combined with mass spectrometry to identify components of protein complexes. Methods Mol Biol 439:309–326
14. Novello F, McLean P (1968) The pentose phosphate pathway of glucose metabolism. Measurement of the non-oxidative reactions of the cycle. Biochem J 107:775–791
15. Wamelink MM, Struys EA, Huck JH, Roos B, van der Knaap MS, Jakobs C, Verhoeven NM (2005) Quantification of sugar phosphate intermediates of the pentose phosphate pathway by LC-MS/MS: application to two new inherited defects of metabolism. J Chromatogr B Analyt Technol Biomed Life Sci 823:18–25
16. Wamelink M, Jansen E, Struys E, Lehrach H, Jakobs C, Ralser M (2009) Quantification of *Saccharomyces cerevisiae* pentose-phosphate pathway intermediates by LC-MS/MS. Nature Protocols Network. doi:10.1038/nprot.2009.140
17. Wamelink MM, Smith DE, Jakobs C, Verhoeven NM (2005) Analysis of polyols in urine by liquid chromatography-tandem mass spectrometry: a useful tool for recognition of inborn errors affecting polyol metabolism. J Inherit Metab Dis 28:951–963
18. Linde L, Kerem B (2008) Introducing sense into nonsense in treatments of human genetic diseases. Trends Genet 24:552–563
19. Cappellini MD, Fiorelli G (2008) Glucose-6-phosphate dehydrogenase deficiency. Lancet 371:64–74
20. Verhoeven NM, Huck JHJ, Roos B, Struys EA, Salomons GS, Douwes AC, van der Knaap MS, Jakobs C (2001) Transaldolase deficiency: liver cirrhosis associated with a new inborn error in the pentose phosphate pathway. Am J Hum Genet 68:1086–1092
21. Wamelink MM, Struys EA, Jakobs C (2008) The biochemistry, metabolism and inherited defects of the pentose phosphate pathway: a review. J Inherit Metab Dis 31:703–717
22. Tylki-Szymanska A, Stradomska TJ, Wamelink MMC, Salomons GS, Taybert J, Pawlowska J, Jakobs C (2009) Transaldolase deficiency in two new patients with a relative mild phenotype. Mol Genet Metab 97:15–17